Alterations in cerebellar grey matter structure and covariance networks in young people with Tourette syndrome

Hilmar P. SIGURDSSON[a*], Stephen R. JACKSON[a,b], Laura JOLLEY[a,†], Ellie MITCHELL[a,†], Georgina M. JACKSON[b].

[a] School of Psychology, University of Nottingham, UK

[b] Institute of Mental Health, School of Medicine, University of Nottingham, UK

[†] These authors contributed equally

[*]Corresponding author

Dr. Hilmar P. SIGURDSSON

Institute of Neuroscience

Newcastle University

Newcastle NE1 7RU

Email: hilmar.sigurdsson@newcastle.ac.uk

ORCID: 0000-0002-0624-065X

1. Abstract

Tourette syndrome (TS) is a childhood-onset neurological disorder characterised by the occurrence of motor and vocal tics and the presence of premonitory sensory/urge phenomena. Functional neuroimaging studies in humans, and experimental investigations in animals, have shown that the genesis of tics in TS involve a complex interaction between cortical-striatal-thalamic-cortical brain circuits and additionally appears to involve the cerebellum. Furthermore, structural brain imaging studies have demonstrated alterations in grey matter (GM) volume in TS across a wide range of brain areas, including alterations in GM volume within the cerebellum. Until now, no study to our knowledge has yet investigated how GM structural covariance networks linked to the cerebellum may be altered in individuals with TS. In this study we employed voxel-based morphometry, and a 'seed-to-voxel' structural covariance network (SCN) mapping approach, to investigate alterations in GM cerebellar volume in people with TS, and alterations in cerebellar SCNs associated with TS. Data from 64 young participants was entered in the final analysis, of which 28 had TS while 36 were age- and sex-matched healthy volunteers. Using the spatially unbiased atlas template of the cerebellum and brainstem (SUIT) atlas, we found reduced GM volume in cerebellar lobule involved in higher-order cognitive functions and sensorimotor processing, in patients. In addition, we found that several areas located in frontal and cingulate cortices and sensorimotor network in addition to subcortical areas show altered structural covariance with our cerebellar seed compared to age-matched controls. These results add to the increasing evidence that cortico-basal ganglia-cerebellar interactions play an important role in tic symptomology.

Keywords: *Tourette syndrome, Cerebellum, Structural Covariance Networks, VBM, sMRI*

2. Introduction

Human brain imaging studies have identified a number of functional brain networks, often referred to as ICNs (intrinsic cortical networks) that reflect correlated brain activity across anatomically separate brain areas. Recent evidence indicates that these networks are dominated by common organizational principles and stable individual features, and largely reflect enduring individual characteristics, including the status of brain health conditions (Gratton et al., 2018). Similarly, neuroimaging studies have repeatedly demonstrated covariance of cortical thickness or grey

matter (GM) volume over widespread, distributed, brain regions, and these structural covariance networks (SCNs) have been shown to be highly heritable and to reflect differences in age and disease status (Alexander-Bloch, Giedd, & Bullmore, 2013). Importantly, it has been proposed that structural covariance between brain regions may reflect brain areas that are functionally co-active; reflect common patterns of maturational change - including shared long-term trophic influences; shared patterns of gene co-expression (Romero-Garcia et al., 2018; Zielinski, Gennatas, Zhou, & Seeley, 2010); and are selectively vulnerable to specific brain health conditions (Seeley, Crawford, Zhou, Miller, & Greicius, 2009). In support of this, recent studies have demonstrated that SCNs closely mirror the functional ICNs revealed using resting-state functional magnetic resonance imaging [fMRI] (C. Kelly et al., 2012; Seeley et al., 2009) and co-degenerate in distinct human neurodegenerative conditions (Cauda et al., 2018; Seeley et al., 2009).

This suggests that analysis of SCNs, while currently under-utilised to study brain networks in neurodevelopmental conditions, may be a particularly useful method for investigating alterations in brain network development in children and adolescents for whom the use of conventional fMRI approaches is especially challenging. In this study we chose to investigate specifically how cerebellar SCNs may be altered in children and adolescents with Tourette syndrome relative to a group of age- and gender-matched typically developing individuals.

Tourette syndrome (TS) is a common neurological disorder of childhood onset that is characterised by the occurrence of vocal and motor tics, and has been associated with alterations in the balance of excitatory and inhibitory signaling within cortical-striatal-thalamic-cortical brain circuits that are implicated in movement selection and habit learning (Albin & Mink, 2006); impaired operation of GABA (inhibitory) signaling within the striatum and cortical motor areas (Gilbert et al., 2004; Kalanithi et al., 2005; Lerner et al., 2012; Orth, Münchau, & Rothwell, 2008; Orth & Rothwell, 2009); and hyper-excitability of limbic and motor cortical regions of the brain that may contribute to the occurrence of tics (Heise et al., 2010; Vaccarino, Kataoka, Yuko, & Lennington, 2013). Nonetheless, there is now increasing evidence to indicate that the cerebellum may play a key role in the pathogenesis of TS and particularly in the release of tics.

The cerebellum occupies only approximately 10% of the total brain volume and contains nearly half of the total number of neurons in the brain (Ramnani, 2006). It is separated into three divisions: the anterior lobe consisting of lobules I-V, the posterior lobe consisting of lobules VI-IX

(lobule VII includes Crus I and lobule VIIb), and the flocculonodular lobe, consisting of lobule X (Stoodley & Schmahmann, 2010). The cerebellum has long been considered to play a central role in the efficient control of movements and in motor learning. Cerebellar damage leads to impairments in motor control and posture, and many efferent projections from the cerebellum are directed to the brain motor system. More recently, however, the cerebellum has also been linked to a variety of non-motor domains including: vestibular and somatosensory function, cognition, and working memory (Buckner, Krienen, Castellanos, Diaz, & Yeo, 2011; Stoodley & Schmahmann, 2009, 2010).

Human neuroimaging studies have confirmed that the cerebellum may play a key role in the execution of tics in TS. Functional magnetic resonance imaging (MRI) and positron emission tomography (PET) studies that have investigated brain activity that immediately precedes, or coincides with, the execution of tics in TS, have repeatedly demonstrated that the cerebellum appears to contribute to tic release (Bohlhalter et al., 2006; Lerner et al., 2007; Neuner et al., 2014). Support for this proposal also comes from a very convincing 'striatal disinhibition' animal model of TS, that has demonstrated that micro-injection of GABA antagonists within the striatum can produce tic-like movements in experimental animals (Bronfeld, Yael, Belelovsky, & Bar-Gad, 2013; McCairn, Bronfeld, Belelovsky, & Bar-Gad, 2009), that are accompanied by the abnormal discharge of cerebellar neurons that immediately precede the release of the tic-like movements (McCairn, Iriki, & Isoda, 2013). Based upon this evidence, it is proposed that the cerebellum may play a specific role in the release of tics (Bohlhalter et al., 2006; Bronfeld et al., 2013; McCairn et al., 2013).

Whole-brain PET imaging studies have reported altered metabolic function of the cerebellar cortex in TS that is characterised by increased resting metabolic activity (Pourfar et al., 2011) and increased GABA-A receptor binding within the cerebellum (Lerner et al., 2012). In addition, MRI studies have demonstrated alterations in GM structure within the cerebellum of individuals with TS relative to a group of matched controls (Tobe et al., 2010). Specifically, it was reported that GM volume in Crus I and lobules VI, VIIb and VIIIa, were reduced bilaterally in the TS group relative to a matched control group. Furthermore, vocal tic severity was found to predict reduced GM volume in both Crus I and lobule VI (Tobe et al., 2010).

Taken together, the above evidence indicates that it may be important to investigate further the potential contribution of the cerebellum to the release of tics and to the pathophysiology of TS

more generally. In this study we use voxel-based morphometry techniques together with seed-based structural covariance analysis methods to investigate: (i) structural alterations in targeted cerebellar lobules (i.e., VI, VIIb and VIIIa and Crus I), based upon the study by Tobe and colleagues (2010) relative to a matched group of typically developing individuals; and (ii) alterations in cerebellar structural covariance networks in the TS group relative to controls.

3. Methods

This study was reviewed and approved by the Nottingham Healthcare foundation trust and the Nottingham Research Ethics committee 1 [Nottingham REC 1]. Written informed consent was acquired from all participants and where appropriate from their parents/caregivers. No part of our study procedures or study analyses were pre-registered prior to the research being conducted. We report how we determined our sample size, all data exclusions, all inclusion/exclusion criteria, whether inclusion/exclusion criteria were established prior to data analysis, all manipulations, and all measures in the study. Finally, due to the conditions of our ethical approval, we are unable to archive individual MRI, clinical biographical data or analysis code under public domains because the data and code contain information that could identify patients. For this reason, MRI, clinical biographical data or analysis code cannot be shared with anyone outside of the research team identified in our ethical approval. There are no other conditions.

3.1. Participants

In total, 76 volunteers took part in this study. 39 had a confirmed diagnosis of TS (TS group) and 37 were closely age- and sex-matched typically developing individuals with no history of neurological disorders. These volunteers formed our control group (CS group). 10 patients with TS had confirmed or suspected clinical diagnosis of a co-occurring condition in addition to their TS (2 attention deficit/hyperactivity disorder [ADHD]; 2 obsessive-compulsive disorder [OCD] and 6 autism spectrum disorder [ASD]). 10 patients were medicated at the time of scanning. Group characteristics are reported in Table 1. Patients were recruited either from the Child and Adolescent Psychiatry Clinic at the Queens Medical Centre in Nottingham or by advertising through the Tourettes Action charity or regional TS support groups. The CS group were recruited from local schools, by local advertising, and recruitment at science fairs. All volunteers were provided with a small inconvenience allowance for their participation.

3.2. Diagnosis, symptom severity and screening

Diagnosis of TS was confirmed by an experienced clinician. Participants recruited outside of the Nottingham area were required to supply information on their condition from their GP or clinical specialist. These participants were also asked to supply information about any other relevant diagnoses and currently prescribed medication.

In addition, all participants underwent comprehensive screening for current symptoms of TS by a highly experienced and trained research nurse. Measures of the current severity of tics were obtained using the Yale Global Tic Severity Scale (YGTSS) (Leckman et al., 1989). The YGTSS is a semi-structured clinician-rated measure assessing the nature of motor and vocal tics present over the past two weeks. The YGTSS consists of three subscales: impairment rating, motor tic rating and vocal tic rating. The current frequency and severity of premonitory sensory/urge phenomena [PSP] was measured using the Premonitory Urge for Tics Scale (PUTS) (Woods, Piacentini, Himle, & Chang, 2005). The PUTS is a self-report measurement where items assess the intensity and frequency of PSP (on a scale of 1 – 4). 9 of the 10 items on the PUTS scaled were scored based on recommendation, and thus scores could range from 9 to 36 (Woods et al., 2005). Participants were screened for any indication of symptoms of ADHD, OCD and Autism using the Connors-3 Parent Report (Conners, 2008), Children's Yale-Brown Obsessive-Compulsive Scale (CY-BOCS) (Scahill et al., 1997) and Social Communication Questionnaire (SCQ) (Berument, Rutter, Lord, Pickles, & Bailey, 1999), respectively. Based on these measures, a further eight patients were categorised as a high risk of having OCD and/or ADHD. All participants also completed the Wechsler's Abbreviated Scale of Intelligence (WASI-II) (Wechsler, 1999) used to assess intellectual ability. Two subtests were used (the verbal and performance subtests). Participants were excluded from the study if their WASI score was < 70.

3.3. MR image acquisition

Whole-brain, high-resolution, T1-weighted structural MRI brain images were acquired for each participant. Scanning was conducted at the Sir Peter Mansfield Imaging Centre (SPMIC), Nottingham, UK using a 3T Philips Achieva MRI scanner with a 32-channel SENSE head-coil and running a MPRAGE sequence (180 contiguous axial slices, 8.1 ms repetition time [TR], 3.7 ms echo time [TE], 256 x 224 x 180 matrix size, flip angle 8°, 1x1x1 mm raw voxel size and scan duration of 225 seconds). Prior to acquisition, participants were asked to lie as still as possible

with their eyes open. Foam padding was added for extra stability and to reduce head movements. All participants wore also noise-cancelling headphones.

3.1. Regions-of-interest

In our study, our voxel-based morphometry [VBM] voxel-wise comparison of local GM cerebellar volume was based on the freely available human cerebellum template and probabilistic atlas [SUIT] (Diedrichsen, 2006; Diedrichsen, Balsters, Flavell, Cussans, & Ramnani, 2009). The SUIT atlas contains 13 bilateral regions of the cerebellum (lobules I-IV, V, Crus I and Crus II, VIIb, VIIIa, VIIIb, IX, X, dentate, interposed nucleus and fastigial nucleus) and vermis containing 8 regions. Based on the SUIT atlas we chose, *a priori,* six regions of interest (ROI) which were combined into a single binary mask consisting of non-zero elements defining our ROIs which was then entered as an explicit mask in our VBM analyses. These ROIs (depicted in Figure 1) consisted of: the bilateral Crus I; and lobules VI; VIIb; and VIIIa, and were chosen based upon their prominent role in sensorimotor processing (Stoodley & Schmahmann, 2009, 2010), their identified role and in tic genesis and execution (Bohlhalter et al., 2006; Lerner et al., 2007; van der Salm et al., 2018), and previously reported differences in previous studies in TS using volumetric measures (Tobe et al., 2010).

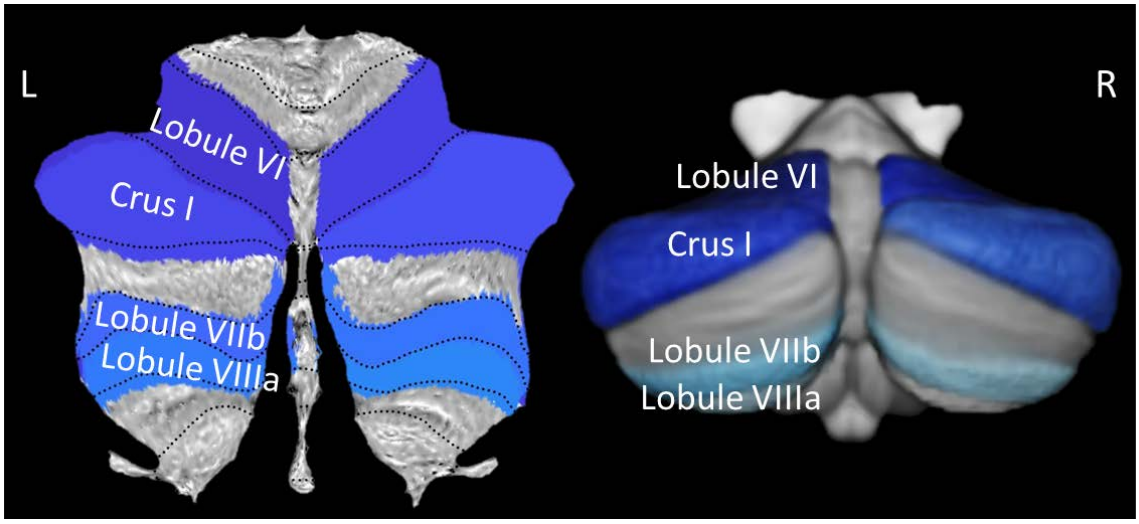

Figure 1. ROIs used in our study: bilateral Crus I and Lobules VI, VIIb and VIIIa. The left image demonstrates our chosen ROIs on a flatmap, whereas the right image demonstrates our ROIs rendered on a segmented template from the SUIT toolbox.

3.2. Isolation of the cerebellar cortex

Raw structural T1-w MRI scans were first oriented to have the origin lying on the AC-PC line using an automated registration process in MATLAB (v. R2017b, The MathWorks Inc., Natick MA, USA). Successful orientation was assessed manually using the 'Display' function in SPM12 (Wellcome Trust Centre for Neuroimaging; http://www.fil.ion.ucl.ac.uk/). All scans were initially preprocessed using the Computational Anatomy Toolbox (CAT12; http://www.neuro.uni-jena.de/cat/, v.6). CAT12 implements a retrospective quality assurance framework for easy quantification of quality of brain images. Each image rated is given a nominal letter from A+ (excellent) to F (unacceptable) by the software to indicate overall quality of the image. All images rated as excellent or good (A+ to B-) were classified as 'high' quality; satisfactory or sufficient (C+ to D-) as 'acceptable' quality; and critical or unacceptable (E+ to F) as 'poor' quality. All images classified as 'poor' were excluded and the 'acceptable' category was then subjected to further careful scrutiny and accepted or rejected as appropriate by the first author (H.P.S).

Using the SUIT toolbox (http://www.diedrichsenlab.org/imaging/suit.htm) the infratentorial structures (i.e., cerebellum and brainstem) were isolated from surrounding tissue and segmented into GM and WM tissue classes using the `suit_isolate_seg` function. The isolated GM maps were inspected visually for any 'leakage' or misclassification and subsequently corrected as necessary. The segmented images showing infratentorial structures were inspected for image quality using MRIcron (https://www.nitrc.org/projects/mricron). Segmented images were normalised to a specific SUIT template using DARTEL (Ashburner, 2007). The segmented and normalised images were resliced into SUIT space using the generated flowfield and affine transformations. The images were modulated to account for any volume changes incurred the normalization step. Finally, all images were smoothed using a 4 mm FWHM (full-width at half maximum) Gaussian kernel (Kühn, Romanowski, Schubert, & Gallinat, 2012). Scans for both groups, in addition to the covariates of no interest, which included de-meaned values of age, total intracranial volume (TIV; the sum of total GM, WM and CSF), IQ and sex (not centered), were entered into a general linear model (GLM) in SPM12. For any given statistical comparison, two group comparisons (contrasts) were tested: TS group > CS group and CS group > TS group. Linear regression analyses were also conducted to investigate positive and negative linear relationships between our covariates of interest (i.e., clinical scores) and cerebellar GM volume values. All corresponding statistical t-maps were thresholded and initially explored at a $p < 0.001$

uncorrected cluster forming peak-level threshold. The spmT maps were then corrected for multiple comparison using the 'Non-stationary cluster extent correction' in CAT12 (Hayasaka, Phan, Liberzon, Worsley, & Nichols, 2004; Worsley, Andermann, Koulis, MacDonald, & Evans, 1999) since VBM violates the assumption of non-isotropic smoothness of the data. T-maps generated from group comparisons and regression analyses of cerebellar GM volume was displayed on flatmaps for better visualization (Diedrichsen & Zotow, 2015). Labelling of significant clusters was accomplished using the thresholded t-maps as overlay on the SUIT atlas in MRIcron.

3.3. Structural covariance

For the structural covariance analysis, all high-quality re-oriented images prior to the cerebellar isolation step (described above) were entered into CAT12 using the 'Segment data' module and the default settings. Precisely, the images were (i) bias and noise-corrected using the Spatially Adaptive Non-Local Means (SANLM) tool (ii) segmented into tissue types (GM, WM and CSF), (iii) spatially normalised to a template in MNI space using DARTEL and affine registration (Ashburner, 2007), (iv) modulated, (v) smoothed using an 8 mm FWHM Gaussian kernel, and (vi) corrected for covariates of no interest (age, IQ, sex and TIV) as outlined above. Then, using the segmented whole-brain GM maps and a 'seed-to-voxel' approach, we computed the structural covariance between the mean GM values for voxels within the Crus I region of the cerebellum (seed) and the GM values for all other voxels in the GM maps. This analysis yielded a covariance map for each group in which the value at each voxel reflected a z-score of covariance between the mean GM value for the seed region and GM value at that particular voxel following a Fisher's r-to-Z transformation:

```
(1)   z1 = 0.5 * log([(1 + r1)/(1 - r1)]);
(2)   z2 = 0.5 * log([(1 + r2)/(1 - r2)]);
```

Where 'r1' and 'r2' represent the cross-subject Pearson correlation coefficient. The whole-brain correlation maps for each group were then statistically compared at group-level using the Z-statistic:

```
(3)   Z = (z1 – z2) / [1/(n1 - 3) + 1/(n2 - 3)]^0.5;
```

Where 'n1' and 'n2' are the total number of participants in the CS and TS groups, respectively. The computed Z-maps were then corrected for multiple comparisons using FDR [p-FDR < 0.05] (Benjamini & Hochberg, 1995) and a cluster threshold of ≥ 100 contiguous voxels was applied. We applied an extent threshold for two reasons; first, Z-maps are corrected for multiple

comparisons at each voxel, and second, an extent threshold of 100 voxels simplified the reporting and interpretation of the SCN results, as well as allowing greater specificity of the relationships between our seed and clusters (see for example Li et al., 2019).

4. Results

4.1. Group characteristics

The quality control investigation of the preprocessed images provided an overall good image quality for majority of the participants. In total, 12 participants were excluded before the final analysis, 1 from the CS group (final N = 36) and 11 from the TS group (final N = 28). One patient with TS was excluded due learning, memory and sight deficits and 2 were excluded due to technical (scanner) error. A further 9 participants were excluded due to excessive image noise or motion artefact (based on the retrospective QA): 1 participant from the CS group and 8 from the TS group. Demographic details of the final sample included in the analyses are shown in Table 1 and Figure 2. Briefly, the groups in the final sample were of statistically comparable in age ($t(62) = -0.28$, $p = 0.78$, age range 9.7 – 22.7 years) however, the CS group had a significantly greater TIV ($t(62) = 2.81$, $p = 0.007$). Importantly, however, the groups demonstrated comparable total volume of the cerebellar cortex ($t(62) = 1.77$, $p = 0.08$). The TS group had lower recorded IQ measured using the WASI ($t(62) = 2.21$, $p = 0.03$) but it should be noted that both groups exhibited above-average mean IQ scores.

Table 1. Summary of group characteristics. Values are displayed as mean (± 1SD).

	Group CS (*n* = 36)	Group TS (*n* = 28)	t/χ2
Age	14.4 ± 3.2	14.6 ± 3.4	-0.28
Sex (M:F)	33:3	25:3	0.11
WASI	118.6 ± 12.3	111.4 ± 13.9	2.21*
TIV	1640.9 ± 158.7 mL	1545.0 ± 97.2 mL	2.81**
Cerebellar volume	117.6 ± 11.1 mL	113.2 ± 7.9 mL	1.77
PUTS scale	-	20.2 ± 6.8	-
Global YGTSS scale	-	33.9 ± 19.3	-
Impairment sub-scale	-	11.3 ± 9.6	
Yale motor tic sub-scale	-	12.9 ± 5.3	-
Yale vocal tic sub-scale	-	10.0 ± 6.7	-

*p < 0.05; ** p < 0.01. Note that clinical measures were only collected from the patient group.

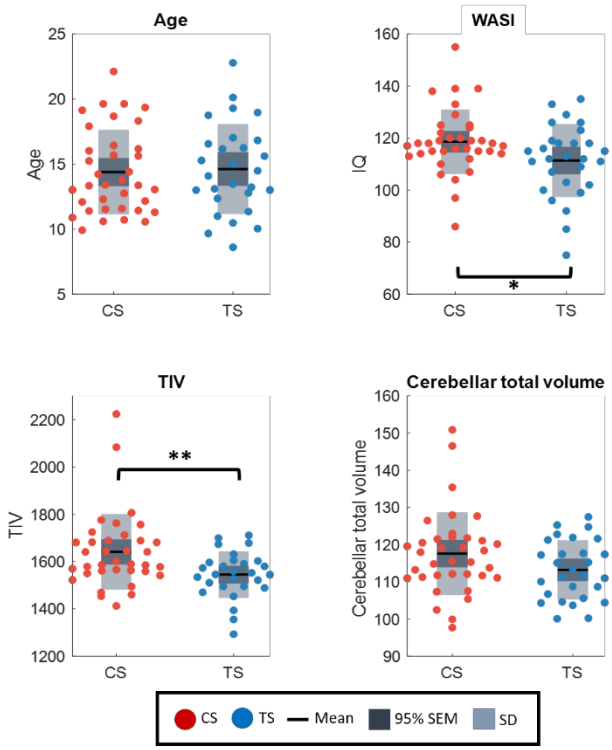

*Figure 2. Comparison of key group characteristics, age, WASI (IQ), TIV and cerebellar volume. Each datapoint represents a single subject (red: CS group, blue: TS group). Dark grey box = 95% SEM, light grey box = SD, black line = group mean. *p < 0.05; **p < 0.01.*

4.2. Group comparison of cerebellar cortex

Statistical comparison of cerebellar GM volume between the two groups yielded significant findings which are summarised in Table 2 and displayed in Figure 3 (which shows the significant clusters along with average individual datapoints extracted from the clusters). In brief, the contrast TS group < CS group revealed a *reduction* of GM volume in cerebellar lobule VIIIa in the right hemisphere and Crus I in the left hemisphere following cluster extent correction. No other cluster survived this stringent correction for multiple comparison, whereas 2 other clusters were observed at the initial cluster-forming uncorrected p < 0.001 thresholds (i.e., left cerebellar lobules VIIb and

VIIIa). The contrast of TS group > CS group returned no statistically significant results (at uncorrected p < 0.001 threshold).

Table 2. The table displays results from our VBM cerebellar GM volume comparison. Clusters were initially formed at a peak-level p < 0.001 threshold and subsequently corrected for multiple comparison using a cluster correction within the CAT12 toolbox.

Cluster	Anatomical label	MNI	#voxels	Peak t-value	p-uncorrected
1	R Lobule VIIIa	6 -70 -47	49	4.56	< 0.001
2	L Crus I	-38 -79 -40	43	3.95	< 0.001

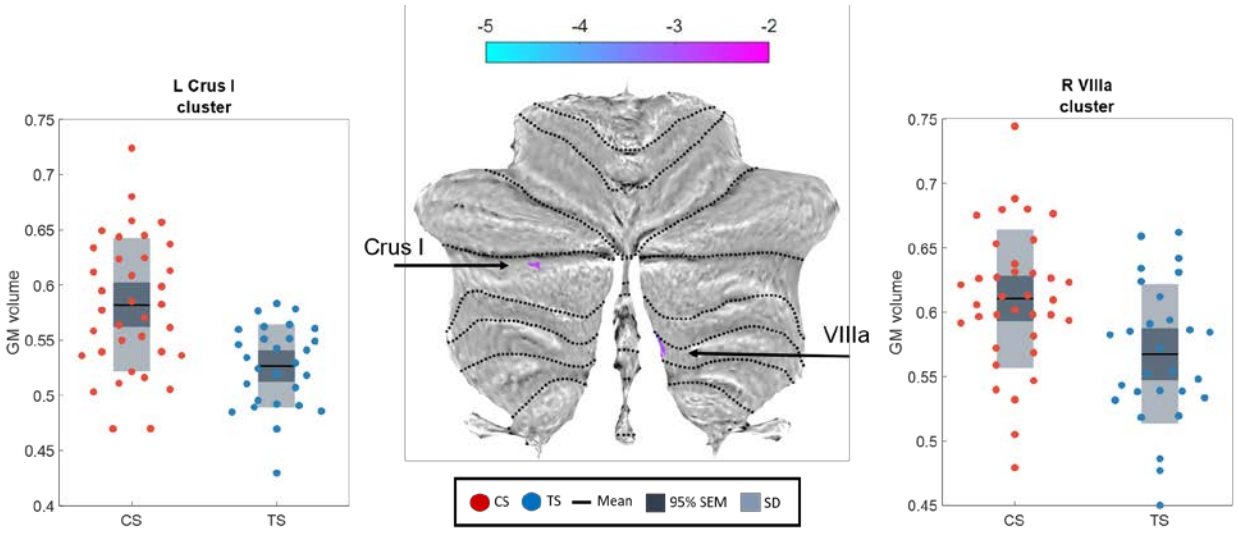

Figure 3. Region showing reduced GM volume in the TS group in comparison to the CS group. The SPM t-map (thresholded at p<0.001) is projected on to a flatmap (right) with individual data points (i.e., extracted as average from each subject within each significant cluster) shown on the left. The colorbar shows the t-statistic.

4.3. Correlation analysis: GM volume and clinical scores

We also conducted a correlation analysis, assessing the relationship between GM values within our cerebellar ROIs and: the PUTS scores; Yale motor and Yale vocal tic subscales; and the Yale

Global Tic Severity scale (global YGTSS). Results are presented in Figure 4 and further outlined in Table 3. In brief, our investigation of positive association between cerebellar GM volume and PUTS scores demonstrated a significant cluster located in the right cerebellar lobule VI following cluster extent correction. No statistically significant clusters were found for the opposite contrast (negative association). By contrast, we found a statistically significant negative association between the Yale motor tic subscale score and cerebellar GM volume in the left cerebellar lobule VI (at $p < 0.001$, MNI: -16 -61 -13), whereas no positive relationship was found. This cluster did, however, not survive a cluster correction. Similarly, no relationship was found between local cerebellar GM volume and Yale Vocal Tic subscale or global scores (all $p > 0.001$).

Table 3. The table lists MNI coordinates and anatomical labels of regions showing statistically significant, positive relationship with PUTS scores.

Cluster	Anatomical label	MNI	#voxels	Peak t-value	p-uncorrected
1	R Lobule VI	31 -50 -32	20	3.88	< 0.001

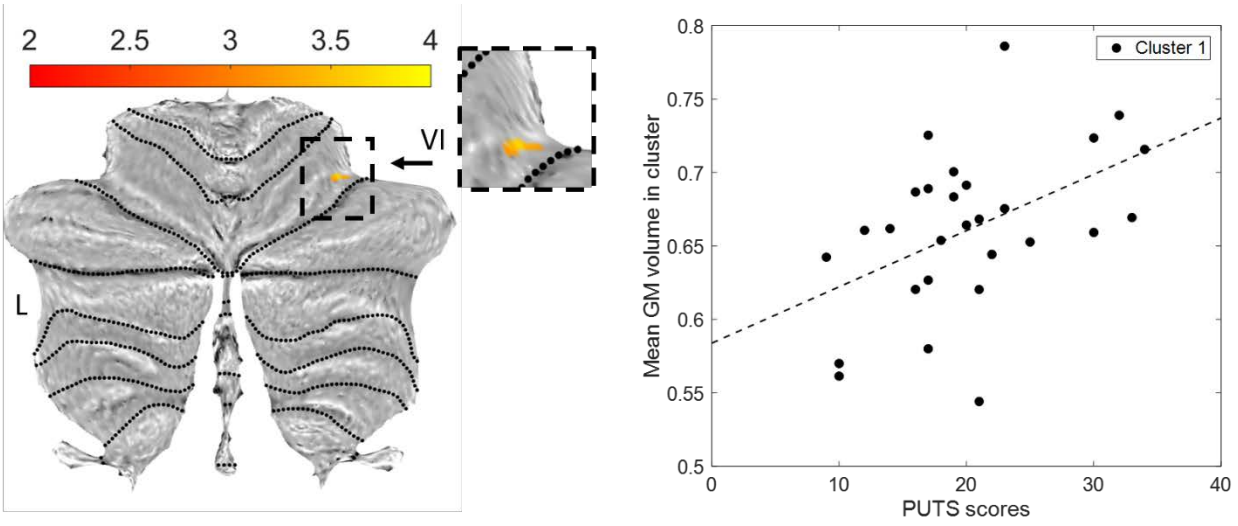

Figure 4. A region showing correlation between PUTS and GM volume in the cerebellum in patients located in the right cerebellar lobule VI. SPM t-map (thresholded at $p < 0.001$) is projected on to a flatmap. The colorbar shows the t-statistic.

4.4. Structural covariance

Our 'seed-to-voxel' structural covariance analysis with Crus I as our seed showed widespread structural covariance with several regions for both groups. Note, for completeness we investigated 'seed-to-voxel' covariance maps for all ROIs depicted in Figure 1 and this resulted in near identical maps for both groups but are not shown or discussed in the present study for brevity.

For the TS group specifically, the Crus I seed showed statistically significant ($p < 0.05$ FDR-corrected) *positive* GM volume correlations with several areas including the subgenual anterior cingulate cortex (sACC), posterior-medial frontal cortex (pMFC; [SMA]), precentral and postcentral gyri, mid-cingulate cortex (MCC) and middle frontal gyrus and statistically significant *negative* correlations with the precuneus and putamen. By contrast, the CS group showed statistically significant ($p < 0.05$ FDR-corrected) *positive* GM volume correlations with the thalamus (somatosensory and parietal sub-regions), cuneus and area TE 3 (superior temporal gyrus) as well as a statistically significant *negative* correlation with the ACC, precentral and postcentral gyri, inferior frontal gyrus (pars opercularis) and middle frontal gyrus. Group specific results are displayed in Figure 5 and further detailed in Tables 4 and 5.

Table 4. Anatomical regions showing positive (+) or negative (-) structural covariance with our Crus I seed in the TS group. All clusters are thresholded at p-FDR < 0.05 at voxel-level and cluster size ≥ 100 voxels.

Cluster	*Anatomical label*	*MNI*	*#voxels*	*Peak z-value*
Structural covariance – Group CS+ contrast				
1	Cerebellum Crus I	-31 -71 -29	11,394	0.92
	Cerebellum Crus I	37 -63 -35		
	L Cerebelum VI	-29 -55 -29		
	L Cerebelum VIII	-15 -67 -39		
2	Postcentral gyrus	29 -43 61	267	0.56
	Superior parietal lobule (Area 5L [SPL])	17 -45 63		
3	Thalamus (Somatosensory)	-25 -19 11	169	0.58
	Thalamus (Parietal)	-27 -23 7		
4	Cuneus	23 -69 25	132	0.52
5	Superior temporal gyrus (Area TE 3)	63 -9 3	104	0.51
Structural covariance – Group CS- contrast				
1	Superior medial gyrus	-11 39 31	786	0.57
	ACC	15 45 15		
	Mid orbital gyrus	-9 47 -11		
	ACC	-3 43 19		

2	Middle occipital gyrus (Area PGp [IPL])	-39 -71 29	557	0.49
3	Fusiform gyrus	23 17 -31	420	0.47
	Medial temporal pole	33 13 -35		
4	Precentral gyrus	45 7 31	322	0.50
	Inferior frontal gyrus (p. Opercularis)	41 11 25		
5	Precentral gyrus	-29 7 37	228	0.55
	Inferior frontal gyrus (p. Opercularis)	-37 3 29		
6	Rectal gyrus	5 37 -27	218	0.50
	Middle orbital gyrus	9 33 -13		
7	Postcentral gyrus	-25 -39 73	184	0.58
8	Precentral gyrus	49 -9 59	180	0.51
9	Middle frontal gyrus	33 49 7	129	0.53
	Superior frontal gyrus	33 59 11		
10	Superior medial gyrus	11 63 27		
11	Postcentral gyrus	67 -15 19	110	0.51
12	Precentral gyrus	-27 -15 57	104	0.52

Table 5. Anatomical regions showing positive (+) or negative (-) structural covariance with our Crus I seed in the CS group. All clusters are thresholded at p-FDR < 0.05 at voxel-level and cluster size ≥ 100 voxels.

Structural covariance – Group TS+ contrast				
Cluster	*Anatomical label*	*MNI*	*#voxels*	*Peak z-value*
1	Cerebellum Crus 1	33 -71 -27	20,159	0.93
	Cerebellum Crus 1	-35 -75 -33		
	Cerebellum lobule IX	-7 -51 -37		
2	Subgenual ACC (sACC)	-3 21 -13	1,928	0.68
	ACC	-9 29 -7		
	Area 33 (part of sACC)	-1 13 -5		
	Thalamus (temporal)	-3 -13 1		
	Thalamus (prefrontal)	11 -19 1		
3	Posterior-medial frontal cortex (pMFC [SMA])	-3 -13 55	1090	0.57
	Area 4a (M1 sub-region)	5 -25 51		
	Paracentral lobule	9 -31 57		
	Precuneus	3 -41 57		
	MCC	9 -39 49		
	MCC	-7 -25 47		
4	Precentral gyrus	-53 5 45	798	0.67
	Postcentral gyrus	-53 -3 39		
	Rolandic operculum	-63 1 11		
5	Superior temporal gyrus (STG)	53 -17 -3	679	0.53
6	Hippocampus	19 -3 -25	565	0.53
	Amygdala	33 -1 -21		

7	Superior medial gyrus	-7 57 33	528	0.64
	Superior frontal gyrus	-23 45 45		
8	Middle frontal gyrus	34 57 31	438	0.54
9	Inferior parietal lobule	39 -51 55	285	0.50
	Inferior parietal sulcus (hIP3)	35 -41 41		
10	Middle occipital gyrus	31 -69 31	246	0.51
11	pMFC/SMA	-3 15 53	227	0.48
12	Supramarginal gyrus	69 -15 25	225	0.46
	Postcentral gyrus	61 -11 25		
13	Inferior parietal lobule (hIP2)	-43 -47 47		
14	Superior frontal gyrus	25 35 47	144	0.47
15	Middle temporal gyrus	-61 -13 -19	143	0.47
Structural covariance – Group TS- contrast				
1	Precuneus	-11 -63 39	979	0.63
	Cuneus	13 -63 21		
	Precuneus	15 -51 23		
2	Superior occipital gyrus (Area hOc4d)	-17 -89 23	359	0.59
	Cuneus	-3 -97 27		
	Calcarine gyrus (hOc1)	3 -97 -1		
3	Putamen	31 -3 13	182	0.50
4	Supramarginal gyrus (Area PFm [IPL])	53 -47 25	163	0.51

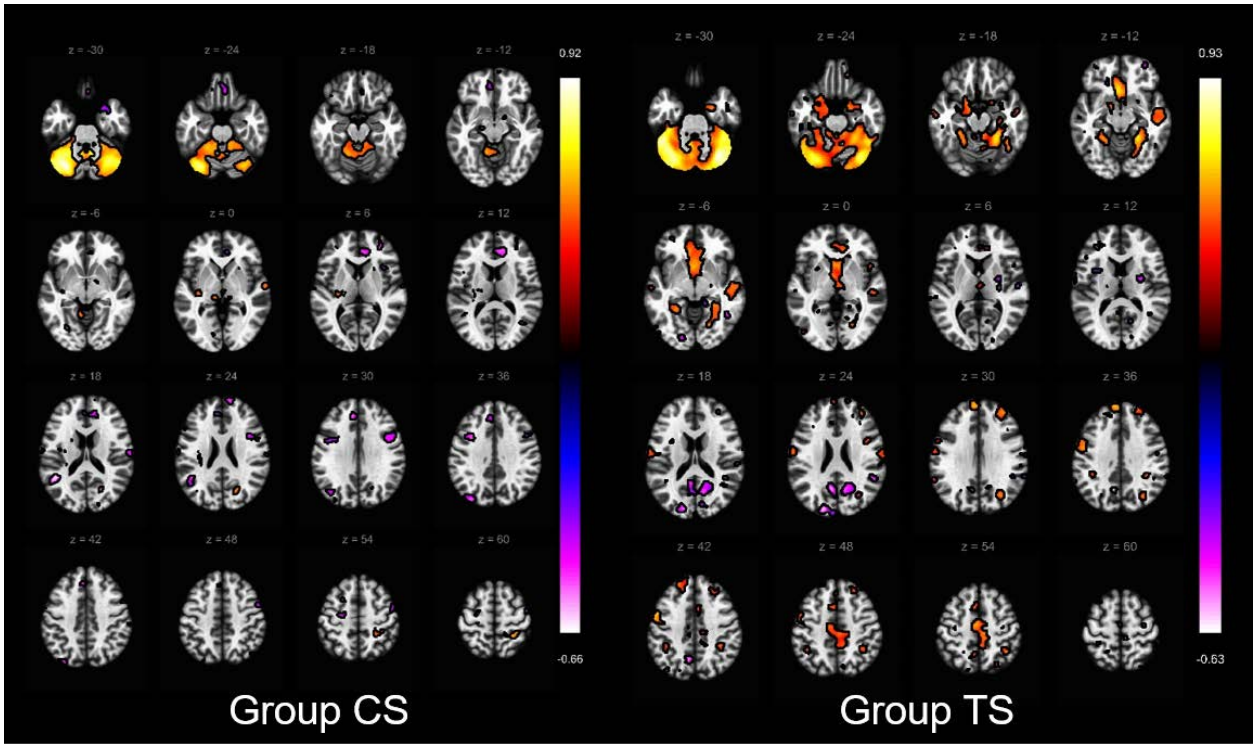

Figure 5. The figure displays results from the analysis of group specific structural covariance networks using a seed-to-voxel approach, with the Crus I as a seed. Left: CS group results; Right: TS group results. Warm (red-yellow) colours demonstrate increased structural covariance, whereas cold (blue-pink) colors demonstrate reduced covariance with our seed. The figure was created using the CONN v18a toolbox (https://web.conn-toolbox.org/).

The TS group > CS group contrast revealed that greater GM volume covariance with the seed region in the cerebellum lobule VI, precentral and postcentral gyri, MCC and subgenual ACC. By contrast, the TS group < CS group contrast demonstrated reduced GM volume covariance in a cluster encompassing the calcarine gyrus and precuneus in the right hemisphere. Results are displayed in Figure 6 and detailed in Table 6.

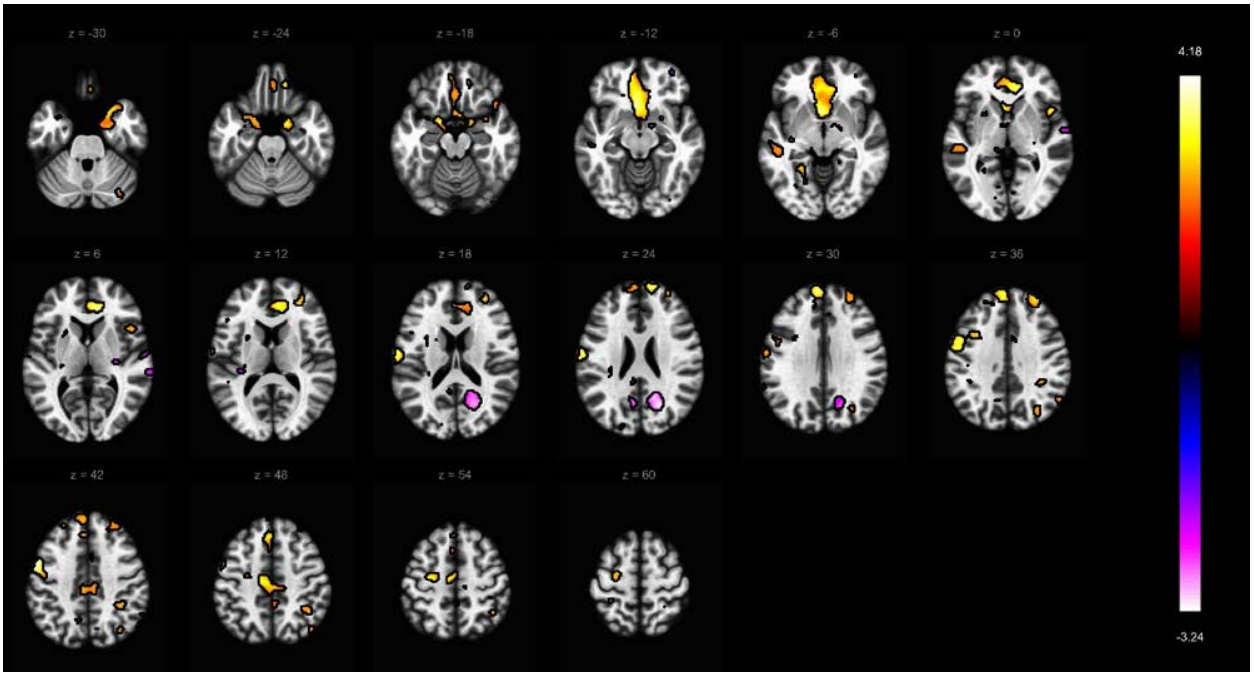

Figure 6. The figure shows results of our between group comparison of structural covariance networks using a seed-to-voxel approach with Crus I as a seed. Warm colors indicate clusters where structural covariance was greater in the TS group (p-FDR < 0.05). By contrast, cold colors indicate clusters where covariance was reduced in the TS group (p-FDR < 0.05).

Table 6. The table details anatomical areas showing significant statistical difference of greater or reduced structural covariance in patients with TS with the Crus I as a seed. All clusters are thresholded at p-FDR < 0.05 at voxel level and cluster size ≥ 100 voxels.

Structural covariance – TS group > CS group contrast				
Cluster	Anatomical label	MNI	#voxels	Peak z-value
1	Area s32 (superior rostral gyrus)	-3 21 -13	3770	3.95
	Superior medial gyrus	-3 59 33		
	Area s24 (subgenual ACC)	-3 15 -5		
	ACC	13 37 7		
	Mid orbital gyrus	-3 33 -9		
2	Cerebellum lobule VI	41 -37 -29	979	3.62
	Hippocampus (CA1)	29 -43 -1		
	Fusiform gyrus (FG4)	51 -47 -27		
	Fusiform gyrus (FG3)	31 -53 -1		
3	Middle temporal gyrus (MTG)	57 -7 -15	745	3.35
	Area TE 3 (superior temporal gyrus)	63 -15 -7		
	Middle frontal gyrus	53 -27 -7		
4	Precentral gyrus	-53 5 45	695	4.18
	Precentral gyrus	-55 -3 41		

	Postcentral gyrus	-65 -9 21		
5	Middle frontal gyrus	31 49 39	517	3.15
	Middle frontal gyrus	33 49 17		
6	Posterior-medial frontal cortex (pMFC)	-9 -17 53	447	3.57
	Middle cingulate cortex (MCC)	-3 -23 47		
7	Postcentral gyrus	69 -15 25	436	3.67
	Supramarginal gyrus	59 -25 43		
8	Precentral gyrus	55 7 45	430	2.94
	Inferior frontal gyrus (IFG)	55 13 35		
	Postcentral gyrus	61 -5 39		
9	Parahippocampal gyrus	-15 3 -19	296	3.47
	Temporal pole	-29 7 -21		
	Amygdala	-29 -3 -21		
10	Middle temporal gyrus (MTG)	-51 -25 1	231	2.50
	Middle temporal gyrus (MTG)	-47 -29 -7		
Structural covariance – TS group < CS group contrast				
1	Calcarine gyrus	21 -65 23	548	3.24
	Precuneus	17 -59 25		

5. Discussion

The primary aim of our study was to investigate whether there were alterations in the structure of areas of the cerebellar cortex targeted *a priori* in a relatively large group of young adults with TS compared to a matched group typically developing volunteers, and further to examine whether there were between-group differences in the structural covariance networks linked to the Crus 1 cerebellar region.

We demonstrated reduced GM volume in the cerebellar lobule Crus I (an area playing a putative role in executive functions) and lobule VIIIa (playing a role in sensorimotor processing) in patients with TS relative to controls when applying our *a priori* chosen ROI cerebellar mask (Buckner et al., 2011; Stoodley & Schmahmann, 2009, 2010). Furthermore, we identified increased GM structural covariance between our Crus I seed region and sensorimotor and frontal cortex areas, MCC and cerebellar lobule VI, as well as reduced covariance with an area encompassing the calcarine gyrus and precuneus.

5.1. Reduced GM volume of several cerebellar areas in TS

Our ROI voxel-wise comparison highlighted several areas of the cerebellum demonstrating GM reduction in patients in comparison with our age- and sex-matched group of healthy volunteer at

uncorrected statistical thresholds. Following a cluster extent correction for multiple comparisons we identified regional reduction of GM volume in cerebellar Crus I and lobule VIIIa in the TS group (Table 2 and Figure 3). This is somewhat consistent with previous findings (Tobe et al., 2010) where reduced bilateral GM portions of the Crus I, in addition to lobules VI and VIIb were reported.

Reciprocal connections of lobules VI, VIIb and VIIIa with the primary motor cortex have been demonstrated in non-human primates (R. M. Kelly & Strick, 2003), and in humans functional neuroimaging studies show that lobule VIIb may play an important role in executive function (Stoodley & Schmahmann, 2009). Lobule VIIIa is activated during motor tasks such as finger tapping (Stoodley & Schmahmann, 2009; Stoodley, Valera, & Schmahmann, 2012) and cutaneous tactile stimulation on the hand and foot (Bushara et al., 2001). This is particularly interesting since patients with TS often report extreme irritation due to the sensation generated by external stimuli, but in the absence of any alterations in sensory thresholds (Belluscio, Jin, Watters, Lee, & Hallett, 2011). The authors suggest that perceived hypersensitivity is due to dysfunctional central processing mechanisms and our results of reduced GM volume in lobule VIIIa are not inconsistent with this proposal. Reciprocal connections between cerebellum and cortex might play an instrumental role in modulating somatosensation, and alterations in cerebellar structure/function may lead to hypersensitivity and the amplified response to sensory input (Koziol, Budding, & Chidekel, 2011; Ramnani, 2006). Further evidence for the role of the cerebellum in sensory sensitivity is demonstrated by children with agenesis of the cerebellum, who exhibit atypical behavioural and emotional response to external sensory input (Koziol et al., 2011).

In our sample of patients with TS, the majority demonstrated symptoms associated with comorbid conditions. In contrast to the study reported by Tobe, et al. (2010), we did not make any TS-related sub-group comparisons of cerebellar GM volume since data from these clinical measures was not collected for all participants, and such analyses would be significantly reduced in statistical power. In their study, Tobe, et al. (2010) compared subgroups of TS+OCD with TS only and found that the differences overlapped with results observed when comparing TS with healthy volunteers but in the opposite direction. That is, local increases of GM volume were observed in lobules VI, VIIb and VIIIa and Crus I. Furthermore, greater hypertrophy was related to OCD disease-related severity (Tobe et al., 2010). In comparison to studies conducted in other clinical samples, we observed some overlap of common cerebellar regions. For example, in children with ASD, D'Mello and colleagues (2015) reported reduced Crus I volume in patients, while bilateral

volume of lobule VI and left Crus I has been demonstrated in medication-naïve adult patients with OCD (Narayanaswamy et al., 2016), where both studies utilized the SUIT atlas. It is therefore possible, based on these studies that reduced volume of Crus I could be related to OCD or ASD in our sample, whereas reduced volume of lobules VIIb (observed at uncorrected $p < 0.001$ only) and VIIIa could be specific to TS. Interestingly, however, increases in TS-related patterns of metabolic activity are observed at rest in cerebellar lobules IV-VI, whereas this pattern is not observed in patients with TS expressing OCD-related symptoms (Pourfar et al., 2011).

5.2. Clinical scores correlate with cerebellar lobule VI

In our analyses we identified two homotopic areas of the cerebellum correlating with clinical measures used in our study (see Figure 4 and Table 3). First, the right lobule VI correlated positively with the PUTS scale. Secondly, the left lobule VI correlated negatively with motor tic scores (observed at uncorrected $p < 0.001$ only). That is, increased motor tic severity was associated with reduced GM volume within lobule VI. We did not observe any significant correlation between global YGTSS score (measuring the global impact of tic symptoms) and GM volume in our cerebellar ROIs. We were also not able to replicate the results of Tobe, et al. (2010), who reported a correlation with the Yale vocal tic scale and GM volume reduction in the Crus I and lobule VI.

In a meta-analysis of cerebellar lobule function, executive function tasks are associated with increased activity in the left lobule VI, while the homologous area on the right seems to play a role in language and working memory (Stoodley & Schmahmann, 2009). Furthermore, lobule VI is functionally related to the somatosensory cerebral network (Buckner et al., 2011; Habas et al., 2009). In TS, metabolic demand increases in lobule VI during tic release (Lerner et al., 2007). Our results from the group comparison provide support for the conclusions drawn by Lerner et al. (2007) who suggested that lobules VI, VIIb and Crus I are involved in tic pathophysiology. We did not identify any volume-related differences in patients relative to controls in lobule VI, and this suggests that GM volume varies only with motor tic or PSP frequency and severity, rather than simply having TS.

The cerebellum is believed to construct internal models (i.e., inverse and forward models), which estimate the dynamic and sensory consequences of a desired action (Wolpert, Miall, & Kawato, 1998). Reduced GM volume in the cerebellum might therefore be related to the difficulty in TS to construct precise internal models since patients have difficulty relying on sensory feedback. This

notion is supported by a recent study by Kim and colleagues (Kim, Jackson, Dyke, & Jackson, 2019) who employed a double-step (reaching towards a target and returning back to starting point) aiming task using a hand-held robot manipulandum and demonstrated that individuals with TS showed particular dysfunction in forward model estimation.

5.3. Structural covariance

In addition to our VBM approach, we investigated structural covariance networks using a 'seed-to-voxel approach, with Crus I as our seed region (see Figure 5 for within group results and Figure 6 for between group results). Crus I is thought to be linked to executive control and shows strong intrinsic functional connectivity with the associative territory of the striatum and the dorsolateral prefrontal cortex (Buckner et al., 2011; Habas et al., 2009). The executive control network is critical for processing information which is important for the preparation for action (Bostan & Strick, 2018). As outlined earlier, correspondence between structural covariance networks and intrinsic functional connectivity networks has been demonstrated in several previous studies (Clos, Rottschy, Laird, Fox, & Eickhoff, 2014; Seeley et al., 2009). Precisely, these studies when employing resting-state or task-based functional MRI in addition to structural covariance using a common area as a seed have shown that connectivity of the seed overlaps significantly between methods and is connected to common networks (Cauda et al., 2018; Clos et al., 2014; Seeley et al., 2009). Furthermore, recent evidence indicates that structural covariance networks may be selectively vulnerable to specific brain health conditions (Cauda et al., 2018; Seeley et al., 2009).

We observed stronger structural covariance between the cerebellar Crus I area and sACC and MCC (the cingulate motor area), bilateral precentral and postcentral gyri, cerebellar lobule VI, and posterior-medial frontal cortex (i.e., SMA) in individuals with TS (see Figure 6). Further, detailed analysis employing multi-modal framework, combining intrinsic functional connectivity and white matter structural connectivity would clarify these results, which show greater covariance between Crus I and the sensorimotor (primary motor and sensory cortices and SMA) and mid-cingulate cortices. Previous volumetric studies of TS have demonstrated reduced GM volume or thickness of the sensorimotor network in young patients with TS (Draper, Jackson, Morgan, & Jackson, 2015; Sowell et al., 2008).

By contrast, we observed reduced structural covariance between Crus I and a cluster encompassing the calcarine gyrus and precuneus in individuals with TS. The precuneus is a critical hub of the default mode network while also playing an important role in the sense of agency

- defined as the sensation of being in control of your actions and their consequences (Farrer et al., 2003). These results are consistent with the proposal that TS is characterized by impaired agency (Delorme et al., 2016)

The involvement of the striatal-thalamic networks in tic genesis and execution has been consistently demonstrated in neuroimaging studies. Specifically, immediately prior to tic onset there is a rise in the fMRI BOLD response in both the putamen and thalamus, as well in the cerebellum (Bohlhalter et al., 2006; Neuner et al., 2014). In both groups we find strong positive covariance between Crus I seed and thalamus, and a negative covariance with the putamen in the TS group only. Animal and computational modelling studies lend further credence to the proposal that basal ganglia and cerebellum networks interact to generate tics (Caligiore, Mannella, Arbib, & Baldassarre, 2017; McCairn et al., 2013).

5.4. Limitations & remarks

First, we recognize that our sample is smaller than that reported by Tobe, et al. (2010) who investigated image acquisitions from 310 individuals of which 163 had TS. Nonetheless, the age range in that study was from 6 to 60 years. As such, we can comfortably say that our study is the largest to date investigating the cerebellar cortex in young (9.7 – 22.7 years) patients with TS and healthy volunteers. We also recognise that the limited availability of information on medication and comorbidities from all patients taking part in our study is a limitation particularly when studying a heterogeneous sample of participants. While we have controlled for several variables such as age, sex, IQ and intracranial volume in our analyses we are not able to provide experimental control of medication dosage or comorbidities, and we interpret our results with this in mind. Studies with larger sample sizes might be able to take these aspects into consideration, particularly since comorbid disorders form a critical aspect of the spectrum of symptoms observed in TS.

Another potential limitation is the clinical characteristics of our TS sample who included individuals with relatively mild tics. Scores for our TS sample had a mean global YGTSS score of 33. Consequently, it is possible that more severely affected patients might have presented with increased structural alterations within the cerebellum. For this reason, we do interpret any null findings or failure to replicate the Tobe et al., (2010) study with caution. Furthermore, patients with greater severity of tics might be excluded due to excessive motion, rendering their images unusable. Head motion during structural MRI acquisition can induce bias in morphometric

analyses. In particular, reduced GM volume has been shown to be influenced by greater head motion (Reuter et al., 2015). Exclusion of images based on visual quality check solely might not be sufficient to prevent this bias (Reuter et al., 2015). Accordingly, we adopted a stringent exclusion criteria while basing our image quality investigation on CAT12 retrospective QA tool in addition to visual checks resulting in exclusion of 9 participants. To further validate our findings, we analysed the results of other cerebellar ROIs as seed regions for our analysis (e.g., lobules VI and VIIIa). This resulted in near identical correlational maps for both groups (data not shown) and for brevity these data are not reported here.

We recognise that we have taken two separate approaches in our analyses (VBM and SCN) to correct our statistical results for multiple testing. Discussion on different multiple testing methods in neuroimaging is beyond the scope of this study, but we would like to emphasise that in both cases we opted not to correct our data with a FWE-correction (e.g., Gaussian random-field theory) since this has been shown to be invalid in settings under non-stationarity (Silver, Montana, & Nichols, 2011). Since structural covariance maps were assessed by correlation between the average GM volume within our seed and every other voxel in the brain we opted to correct our resulting Z maps with an FDR correction at voxel-level and restrict results large clusters to allow for greater spatial specificity. By contrast, we opted for a cluster-extent correction in our VBM analyses while accounting for the non-stationary (i.e., non-uniform) smoothness in the data (Ashburner & Friston, 2000; Hayasaka et al., 2004). Employing two different correction methods, in addition to differences in smoothing kernels between the methods was a judicious decision but can be seen as a limitation in our study. The focus of the current study prevents us from exploring this potential limitation further.

Finally, throughout this paper we have assumed that structural covariance networks (SCNs) closely mirror the intrinsic connectivity networks (ICNs) measured and robustly demonstrated using resting-state fMRI. This assumption is based upon a number of studies, referred to above, that have directly compared seed-based SCNs and ICNs. However, given that our study investigates SCNs in adolescents and young adults with TS – a period during which the brain is known to undergo considerable maturation – it is possible that during this period there could be differences in the maturation of structural and functional brain networks, and that these may be exacerbated by the presence of TS. For this reason, and as we have not directly measured functional brain connectivity in this study, we advocate caution in drawing strong conclusions about functional connectivity based upon our findings of structural covariance differences in TS.

6. Conclusion

Classic theories dictate that the pathophysiology of TS is the result of altered function and structure of several, overlapping cortico-striatal networks. Recent evidence seems to suggest that the cerebellum might play an important role in tic symptomology. In this study, we employed a cerebellar specific template (SUIT) and measured GM volume in young people with TS and matched healthy volunteers. Our results seem to suggest reduced GM volume of several cerebellar lobule which play a pivotal role in sensorimotor and executive function. Furthermore, we showed altered covariance of the cerebellar Crus I seed with sensorimotor, parietal and basal ganglia regions of the cerebral cortex in patients. Our results provide further evidence for the idea that cerebellar-basal ganglia-cortical networks play a prominent role in TS. We urge further studies to explore functional and structural connectivity of the cerebellum in patients with TS.

7. Acknowledgments

This work was supported by the Medical Research Council (grant number G0901321), the James Tudor Foundation, Tourettes Action (UK), and by the NIHR Nottingham Biomedical Research Centre. The views expressed are those of the authors and not necessarily those of the NHS, the NIHR or the Department of Health. The authors would like to thank Jane Fowlie and Tourettes Action (UK) for assisting with participant recruitment.

8. References

Albin, R. L., & Mink, J. W. (2006). Recent advances in Tourette syndrome research. *Trends in Neurosciences*, *29*(3), 175–182. https://doi.org/10.1016/j.tins.2006.01.001

Alexander-Bloch, A., Giedd, J. N., & Bullmore, E. T. (2013). Imaging structural co-variance between human brain regions. *Nature Reviews Neuroscience*, *14*(5), 322–335. https://doi.org/10.1038/nrn3465

Ashburner, J. (2007). A fast diffeomorphic image registration algorithm. *NeuroImage*, *38*(1), 95–113. https://doi.org/10.1016/j.neuroimage.2007.07.007

Ashburner, J., & Friston, K. J. (2000). Voxel-based morphometry - the methods. *NeuroImage*, *11*(6 Pt 1), 805–821. https://doi.org/10.1006/nimg.2000.0582

Belluscio, B. A., Jin, L., Watters, V., Lee, T. H., & Hallett, M. (2011). Sensory sensitivity to external stimuli in Tourette syndrome patients. *Movement Disorders*, *26*(14), 2538–2543. https://doi.org/10.1002/mds.23977

Benjamini, Y., & Hochberg, Y. (1995). Controlling the False Discovery Rate: A Practical and Powerful Approach to Multiple Testing. *Journal of the Royal Statistical Society*, *57*(1), 289–300.

Berument, S. K., Rutter, M., Lord, C., Pickles, A., & Bailey, A. (1999). Autism screening questionnaire: diagnostic validity. *British Journal of Psychiatry*, *175*, 444–451. https://doi.org/10.1192/bjp.175.5.444

Bohlhalter, S., Goldfine, A., Matteson, S., Garraux, G., Hanakawa, T., Kansaku, K., … Hallett, M. (2006). Neural correlates of tic generation in Tourette syndrome: an event-related functional MRI study. *Brain*, *129*, 2029–2037. https://doi.org/10.1093/brain/awl050

Bostan, A. C., & Strick, P. L. (2018). The basal ganglia and the cerebellum: nodes in an integrated network. *Nature Reviews Neuroscience*, 1–13. https://doi.org/10.1038/s41583-018-0002-7

Bronfeld, M., Yael, D., Belelovsky, K., & Bar-Gad, I. (2013). Motor tics evoked by striatal disinhibition in the rat. *Frontiers in Systems Neuroscience*, *7*(50), 1–10. https://doi.org/10.3389/fnsys.2013.00050

Buckner, R. L., Krienen, F. M., Castellanos, A., Diaz, J. C., & Yeo, B. T. T. (2011). The organization of the human cerebellum estimated by intrinsic functional connectivity. *Journal of Neurophysiology*, *106*(5), 2322–2345. https://doi.org/10.1152/jn.00339.2011

Bushara, K. O., Wheat, J. M., Khan, A., Mock, B. J., Turski, P. A., Sorenson, J., & Brooks, B. R. (2001). Multiple tactile maps in the human cerebellum. *NeuroReport*, *12*(11), 2483–2486. https://doi.org/10.1097/00001756-200108080-00039

Caligiore, D., Mannella, F., Arbib, M. A., & Baldassarre, G. (2017). Dysfunctions of the basal ganglia-cerebellar-cortical system produce motor tics in Tourette syndrome. *PLOS Computational Biology*, *13*(3), e1005395. https://doi.org/10.1371/journal.pcbi.1005395

Cauda, F., Nani, A., Manuello, J., Premi, E., Palermo, S., Tatu, K., … Costa, T. (2018). Brain structural alterations are distributed following functional, anatomic and genetic connectivity. *Brain*, *141*(11), 3211–3232. https://doi.org/10.1093/brain/awy252

Clos, M., Rottschy, C., Laird, A. R., Fox, P. T., & Eickhoff, S. B. (2014). Comparison of structural covariance with functional connectivity approaches exemplified by an investigation of the left anterior insula. *NeuroImage*, *99*(1), 269–280. https://doi.org/10.1016/j.neuroimage.2014.05.030

Conners, C. K. (2008). *The Conners 3rd Edition (Conners 3)*. North Tonawanda: Multi-Health system.

D'Mello, A. M., Crocetti, D., Mostofsky, S. H., & Stoodley, C. J. (2015). Cerebellar gray matter and lobular volumes correlate with core autism symptoms. *NeuroImage: Clinical*, *7*, 631–639. https://doi.org/10.1016/j.nicl.2015.02.007

Delorme, C., Salvador, A., Voon, V., Roze, E., Vidailhet, M., Hartmann, A., & Worbe, Y. (2016). Illusion of agency in patients with Gilles de la Tourette syndrome. *Cortex*, *77*(April), 132–140. https://doi.org/10.1016/j.cortex.2016.02.003

Diedrichsen, J. (2006). A spatially unbiased atlas template of the human cerebellum. *Neuroimage*, *33*(1), 127–138. https://doi.org/10.1016/j.neuroimage.2006.05.056

Diedrichsen, J., Balsters, J. H., Flavell, J., Cussans, E., & Ramnani, N. (2009). A probabilistic MR atlas of the human cerebellum. *NeuroImage*, *46*(1), 39–46. https://doi.org/10.1016/j.neuroimage.2009.01.045

Diedrichsen, J., & Zotow, E. (2015). Surface-based display of volume-averaged cerebellar imaging data. *PLoS ONE*, *10*(7), 1–18. https://doi.org/10.1371/journal.pone.0133402

Draper, A., Jackson, G. M., Morgan, P. S., & Jackson, S. R. (2015). Premonitory urges are associated with decreased grey matter thickness within the insula and sensorimotor cortex in young people with Tourette syndrome. *Journal of Neuropsychology*, *10*(1), 143–153. https://doi.org/10.1111/jnp.12089

Farrer, C., Franck, N., Georgieff, N., Frith, C. D., Decety, J., & Jeannerod, M. (2003). Modulating the experience of agency: A positron emission tomography study. *NeuroImage*, *18*(2), 324–333. https://doi.org/10.1016/S1053-8119(02)00041-1

Gilbert, D. L., Bansal, A. S., Sethuraman, G., Sallee, F. R., Zhang, J., Lipps, T., & Wassermann, E. M. (2004). Association of cortical disinhibition with tic, ADHD, and OCD severity in Tourette syndrome. *Movement Disorders*, *19*(4), 416–425.

https://doi.org/10.1002/mds.20044
Gratton, C., Laumann, T. O., Nielsen, A. N., Greene, D. J., Gordon, E. M., Gilmore, A. W., … Petersen, S. E. (2018). Functional brain networks are dominated by stable group and individual factors, not cognitive or daily variation. *Neuron*, *98*(2), 439–452. https://doi.org/10.1016/j.neuron.2018.03.035
Habas, C., Kamdar, N., Nguyen, D., Keller, K., Beckmann, C. F., Menon, V., & Greicius, M. D. (2009). Distinct Cerebellar Contributions to Intrinsic Connectivity. *The Journal of Neuroscience*, *29*(26), 8586–8594. https://doi.org/10.1523/JNEUROSCI.1868-09.2009
Hayasaka, S., Phan, K. L., Liberzon, I., Worsley, K. J., & Nichols, T. E. (2004). Nonstationary cluster-size inference with random field and permutation methods. *NeuroImage*, *22*(2), 676–687. https://doi.org/10.1016/j.neuroimage.2004.01.041
Heise, K. F., Steven, B., Liuzzi, G., Thomalla, G., Jonas, M., Müller-Vahl, K., … Hummel, F. C. (2010). Altered modulation of intracortical excitability during movement preparation in Gilles de la Tourette syndrome. *Brain*, *133*(2), 580–590. https://doi.org/10.1093/brain/awp299
Kalanithi, P. S., Zheng, W., Kataoka, Y., DiFiglia, M., Grantz, H., Saper, C. B., … Vaccarino, F. M. (2005). Altered parvalbumin-positive neuron distribution in basal ganglia of individuals with Tourette syndrome. *Proceedings of the National Academy of Sciences of the United States of America*, *102*(37), 13307–13312. https://doi.org/10.1073/pnas.0502624102
Kelly, C., Toro, R., Di Martino, A., Cox, C. L., Bellec, P., Castellanos, F. X., & Milham, M. P. (2012). A convergent functional architecture of the insula emerges across imaging modalities. *NeuroImage*, *61*(4), 1129–1142. https://doi.org/10.1016/j.neuroimage.2012.03.021
Kelly, R. M., & Strick, P. L. (2003). Cerebellar loops with motor cortex and prefrontal cortex of a nonhuman primate. *The Journal of Neuroscience*, *23*(23), 8432–8444. https://doi.org/10.1523/jneurosci.23-23-08432.2003
Kim, S., Jackson, G. M., Dyke, K. S., & Jackson, S. R. (2019). Impaired forward model updating in young adults with Tourette syndrome. *Brain*, *142*(1), 209–219. https://doi.org/10.1093/brain/awy306
Koziol, L. F., Budding, D. E., & Chidekel, D. (2011). Sensory integration, sensory processing, and sensory modulation disorders: Putative functional neuroanatomic underpinnings. *Cerebellum*, *10*(4), 770–792. https://doi.org/10.1007/s12311-011-0288-8
Kühn, S., Romanowski, A., Schubert, F., & Gallinat, J. (2012). Reduction of cerebellar grey matter in Crus I and II in schizophrenia. *Brain Structure and Function*, *217*(2), 523–529. https://doi.org/10.1007/s00429-011-0365-2
Leckman, J. F., Riddle, M. A., Hardin, M. T., Ort, S. I., Swartz, K. L., Stevenson, J., & Cohen, D. J. (1989). The Yale Global Tic Severity Scale: initial testing of a clinician-rated scale of tic severity. *Journal of the American Academy of Child and Adolescent Psychiatry*, *28*(4), 566–573. https://doi.org/10.1097/00004583-198907000-00015
Lerner, A., Bagic, A., Boudreau, E. A., Hanakawa, T., Pagan, F., Mari, Z., … Hallett, M. (2007). Neuroimaging of neuronal circuits involved in tic generation in patients with Tourette syndrome. *Neurology*, *68*(23), 1979–1987. https://doi.org/10.1212/01.wnl.0000264417.18604.12
Lerner, A., Bagic, A., Simmons, J. M., Mari, Z., Bonne, O., Xu, B., … Hallett, M. (2012). Widespread abnormality of the γ-aminobutyric acid-ergic system in Tourette syndrome. *Brain*, *135*(6), 1926–1936. https://doi.org/10.1093/brain/aws104
Li, K., Luo, X., Zeng, Q., Huang, P., Shen, Z., Xu, X., … Zhang, M. (2019). Gray matter structural covariance networks changes along the Alzheimer's disease continuum. *NeuroImage: Clinical*, *23*(April), 101828. https://doi.org/10.1016/j.nicl.2019.101828
McCairn, K. W., Bronfeld, M., Belelovsky, K., & Bar-Gad, I. (2009). The neurophysiological

correlates of motor tics following focal striatal disinhibition. *Brain*, *132*(8), 2125–2138. https://doi.org/10.1093/brain/awp142

McCairn, K. W., Iriki, A., & Isoda, M. (2013). Global dysrhythmia of cerebro-basal ganglia-cerebellar networks underlies motor tics following striatal disinhibition. *The Journal of Neuroscience*, *33*(2), 697–708. https://doi.org/10.1523/JNEUROSCI.4018-12.2013

Narayanaswamy, J. C., Jose, D., Kalmady, S. V., Agarwal, S. M., Janardhan Reddy, Y. C., Agarwal, S. M., … Janardhan Reddy, Y. C. (2016). Cerebellar volume deficits in medication-naïve obsessive compulsive disorder. *Psychiatry Research: Neuroimaging*, *254*, 164–168. https://doi.org/10.1016/j.pscychresns.2016.07.005

Neuner, I., Werner, C. J., Arrubla, J., Stöcker, T., Ehlen, C., Wegener, H. P., … Shah, N. J. (2014). Imaging the where and when of tic generation and resting state networks in adult Tourette patients. *Frontiers in Human Neuroscience*, *8*, 1–16. https://doi.org/10.3389/fnhum.2014.00362

Orth, M., Münchau, A., & Rothwell, J. C. (2008). Corticospinal system excitability at rest is associated with tic severity in Tourette Syndrome. *Biological Psychiatry*, *64*(3), 248–251. https://doi.org/10.1016/j.biopsych.2007.12.009

Orth, M., & Rothwell, J. C. (2009). Motor cortex excitability and comorbidity in Gilles de la Tourette syndrome. *Journal of Neurology, Neurosurgery, and Psychiatry*, *80*(1), 29–34. https://doi.org/10.1136/jnnp.2008.149484

Pourfar, M., Feigin, A., Tang, C. C., Carbon-Correll, M., Bussa, M., Budman, C., … Eidelberg, D. (2011). Abnormal metabolic brain networks in Tourette syndrome. *Neurology*, *76*(11), 944–952. https://doi.org/10.1212/WNL.0b013e3182104106

Ramnani, N. (2006). The primate cortico-cerebellar system: Anatomy and function. *Nature Reviews Neuroscience*, *7*(7), 511–522. https://doi.org/10.1038/nrn1953

Reuter, M., Tisdall, M. D., Qureshi, A., Buckner, R. L., van der Kouwe, A. J. W., & Fischl, B. (2015). Head motion during MRI acquisition reduces gray matter volume and thickness estimates. *NeuroImage*, *107*, 107–115. https://doi.org/10.1016/j.neuroimage.2014.12.006

Romero-Garcia, R., Whitaker, K. J., Váša, F., Seidlitz, J., Shinn, M., Fonagy, P., … Vértes, P. E. (2018). Structural covariance networks are coupled to expression of genes enriched in supragranular layers of the human cortex. *NeuroImage*, *171*, 256–267. https://doi.org/10.1016/j.neuroimage.2017.12.060

Scahill, L. D., Riddle, M. A., McSwiggin-Hardin, M., Ort, S. I., King, R. A., Goodman, W. K., … Leckman, J. F. (1997). Children's Yale-Brown Obsessive Compulsive Scale: Reliability and Validity. *Journal of the American Academy of Child and Adolescent Psychiatry*, *36*(6), 844–852. https://doi.org/http://dx.doi.org/10.1097/00004583-199706000-00023

Seeley, W. W., Crawford, R. K., Zhou, J., Miller, B. L., & Greicius, M. D. (2009). Neurodegenerative diseases target large-scale human brain networks. *Neuron*, *62*(1), 42–52. https://doi.org/10.1016/j.neuron.2009.03.024.

Silver, M., Montana, G., & Nichols, T. E. (2011). False positives in neuroimaging genetics using voxel-based morphometry data. *NeuroImage*, *54*(2), 992–1000. https://doi.org/10.1016/j.neuroimage.2010.08.049

Sowell, E. R., Kan, E., Yoshii, J., Thompson, P. M., Bansal, R., Xu, D., … Peterson, B. S. (2008). Thinning of sensorimotor cortices in children with Tourette syndrome. *Nature Neuroscience*, *11*(6), 637–639. https://doi.org/10.1038/nn.2121

Stoodley, C. J., & Schmahmann, J. D. (2009). Functional topography in the human cerebellum: A meta-analysis of neuroimaging studies. *NeuroImage*, *44*(2), 489–501. https://doi.org/10.1016/j.neuroimage.2008.08.039

Stoodley, C. J., & Schmahmann, J. D. (2010). Evidence for topographic organization in the cerebellum of motor control versus cognitive and affective processing. *Cortex*, *46*(7), 831–

844. https://doi.org/10.1016/j.cortex.2009.11.008
Stoodley, C. J., Valera, E. M., & Schmahmann, J. D. (2012). Functional topography of the cerebellum for motor and cognitive tasks: An fMRI study. *NeuroImage*, *59*(2), 1560–1570. https://doi.org/10.1016/j.neuroimage.2011.08.065
Tobe, R. H., Bansal, R., Xu, D., Hao, X., Liu, J., Sanchez, J., & Peterson, B. S. (2010). Cerebellar morphology in Tourette syndrome and Obsessive-compulsive disorder. *Annals of Neurology*, *67*(4), 479–487. https://doi.org/10.1002/ana.21918
Vaccarino, F. M., Kataoka, Yuko, & Lennington, J. B. (2013). Cellular and Molecular Pathology in Tourette Syndrome. In D. Martino & J. F. Leckman (Eds.), *Tourette Syndrome*. Oxford University Press.
van der Salm, S. M. A., Van der Meer, J. N., Cath, D. C., Groot, P. F. C., van der Werf, Y. D., Brouwers, E., … Tijssen, M. A. J. (2018). Distinctive tics suppression network in Gilles de la Tourette syndrome distinguished from suppression of natural urges using multimodal imaging. *NeuroImage: Clinical*, *20*, 783–792. https://doi.org/10.1016/j.nicl.2018.09.014
Wechsler, D. (1999). *Wechsler Abbreviated Scale of Intelligence*. San Antonio TX: The Psychological Corporation.
Wolpert, D. M., Miall, R. C., & Kawato, M. (1998). Internal models in the cerebellum. *Trends in Cognitive Sciences*, *2*(9), 338–347. https://doi.org/https://doi.org/10.1016/S1364-6613(98)01221-2
Woods, D. W., Piacentini, J. C., Himle, M. B., & Chang, S. (2005). Premonitory Urge for Tics Scale (PUTS): initial psychometric results and examination of the premonitory urge phenomenon in youths with Tic disorders. *Journal of Developmental & Behavioral Pediatrics*, *26*(6), 397–403.
Worsley, K. J., Andermann, M., Koulis, T., MacDonald, D., & Evans, A. C. (1999). Detecting changes in nonisotropic images. *Human Brain Mapping*, *8*(2–3), 98–191.
Zielinski, B. A., Gennatas, E. D., Zhou, J., & Seeley, W. W. (2010). Network-level structural covariance in the developing brain. *Proceedings of the National Academy of Sciences of the United States of America*, *107*(42), 18191–18196. https://doi.org/10.1073/pnas.1003109107